Supplementary Materials and Methods

Plant material, threshing and growth conditions

Threshing was performed by hand and by the same person to gauge the threshability of mutant wheat lines. In reference to the loss-of-function mutant *Q'-Rev1* threshing required the identification of individual grain for removal by splitting apart florets and spikelets whereas in *Q'* and SS-like spikes, grain could easily be separated by rolling the spike back and forth between clapped palms.

The compact mutant near isogenic lines ANBW5B (5B D in Fig 3) and ANBW5C (5C D in Figure 3) were isolated and mapped by (Kosuge et al., 2011). The lines were established by backcrossing the mutants Cp-M808 (ANBW5B) and MCK 2617 (ANBW5C) with Novosibirskaya 67 (N67) for six generations. N67 contains the typical domesticated *Q* allele. The line 5C T included in Figure 3 represents an N67-like segregant from a line heterozygous for the ANBW5C mutation after backcrossing, however by this round of backcrossing N67 and N67-like segregants are effectively genetically identical.

Screening of mutant lines and phenotyping for co-segregation analysis was performed in glasshouse conditions with temperature controlled to ~22°C (Day) and ~16°C (Night) over Spring and Summer. All other phenotyping and tissue extraction for RNA was from plants grown in cabinets (Conviron PGC20) under 16h light (Measured at 420µM m^{-1} s^{-1} 50cm below light source) (22°C) and 8h dark (16°C).

Modified 5' RACE

mRNA was purified from the same inflorescence RNA samples used for the initial qRT-PCR analysis of *Q* in SS-like and *Q'* plants (Fig 2). A Gene-racer kit (Invitrogen) was used for 5'-RACE, except the de-capping protocol was not carried out, and the adapter was ligated directly to mRNA. Amplification of cleaved and ligated *Q* transcript was performed using gene specific and Gene-racer specific primers. Secondary nested PCR was performed to ensure amplification of gene specific products. Amplification products were gel purified and ligated into pGEM®-T easy before being transformed into *E.coli* XL-Blue cells and selected on ampicillin plates containing 100 µL of 100mM IPTG and 20 µL of 50 mg/ml X-Gal. Individual colonies were selected and grown overnight in LB with 50 µg/ml ampicillin and purified using Qiagen mini-preps. In total, 96 colonies were selected for sequencing of *Q'* (n=48) and SS-like (n=48) amplification product. Only sequenced clones containing correct *Q* transcript sequence were included with the proportion of cleavage within the miR172-binding site presented. Gene specific primer sequences are listed in Supplementary Table 1.

qRT-PCR

All tissue was ground to fine powder in 1.5ml snap lock tubes containing two ball bearings using a mixermill. RNA extraction and DNASE treatment was performed using the Maxwell® RSC Plant RNA Kit and Maxwell® RSC Instrument following the advised protocol. cDNA synthesis was performed using Maxima H-minus reverse transcriptase from invitrogen with oligo dT to prime mRNA using 5µg total RNA. cDNA was diluted 30 fold and 5µl of diluted cDNA was used in each qPCR reaction. qPCR was performed using SYBR Green on a Roche LightCycler®480II using RP15 as an endogenous control. Primers are shown in Supplementary Table S1.

Routine testing of cDNA samples was performed by serial dilution and calculation of R^2 from the standard curve. Analysis was performed using Roche LightCycler®480II and associated software. For all cDNA samples presented, 5 log serial dilutions were performed and R^2 values ≥0.982 were determined before qPCR analysis. Primer efficiency was calculated from the exponential phase of amplification in each reaction sample in each qRT-PCR run. qRT-PCR Primer pairs used in this study routinely achieved amplification efficiencies ≥90%.

Scanning Electron Microscopy (SEM)

Developing inflorescence samples for SEM were prepared by immediate transfer to 100% ethanol after harvest. Ethanol was replaced twice daily until samples appeared completely white (2-3 days). Sample preparation adapted from (Talbot and White, 2013). Samples were then put through a critical point drying process in a tousimis autosamdri®-815 critical point drying device with purge timer set to 4. After critical point drying, samples were mounted on specimen stubs using adhesive carbon discs. Samples were imaged with a Zeiss Evo LS15 scanning electron microscope using backscattered electron detector (Gain= High), at 20KV and extended pressure setting (10pa).

Supplementary Table S1. Primers used in this study

Primer Name	Purpose	Sequence	
pJG31	*Q* Full genomic sequence	GATGGTGCTGGATCTCAATGTGG	
PJG33	*Q* Full genomic sequence	CAACAATGGCGGACTGCTG	
pJG14	*Q* genomic sequence spanning miRNA-Binding site	TCACTGCTGGTGCTGGTGC	
PJG18	*Q* genomic sequence spanning miRNA-Binding site	AAGTAGAACCGGTGGTGGTCC	
pJG38	Sequencing *Q*	CTACGAGGAGGATTTGAAGCAG	
pJG39	Sequencing *Q*	ACACGACACTCGATTGCAGAC	
pJG5	Sequencing *Q*	AATGAGGGTACTACTACAATCGGTC	
pJG2	Sequencing *Q*	CTACCCGAACGTACAGGTATCA	
pJG13	Sequencing *Q*	GGTGCAGGAGAGGCCCAT	
pJG29	*Q* specific 5' Race	GGAAGTAGAACCGGTGGTGGTCC	
pJG30	*Q* specific 5' Race Nested	GTGGTGGTCCGGGTACGGC	
Q qPCR F	*Q* qPCR	CCCTGAATCGTCAACCACAATG	(Simons et al., 2006)
Q qPCR R	*Q* qPCR	CCGTGCCATGTTGATGCA	(Simons et al., 2006)
TaRP15 F	Control gene qPCR	GCACACGTGCTTTGCAGATAAG	(Shaw et al., 2012)
TaRP15 R	Control gene qPCR	GCCCTCAAGCTCAACCATAACT	(Shaw et al., 2012)

miR172 Reverse transcription, expression, control primers associated methods used in this study can be found in companion paper Debernardi et al., 2017.

Supplementary Figures

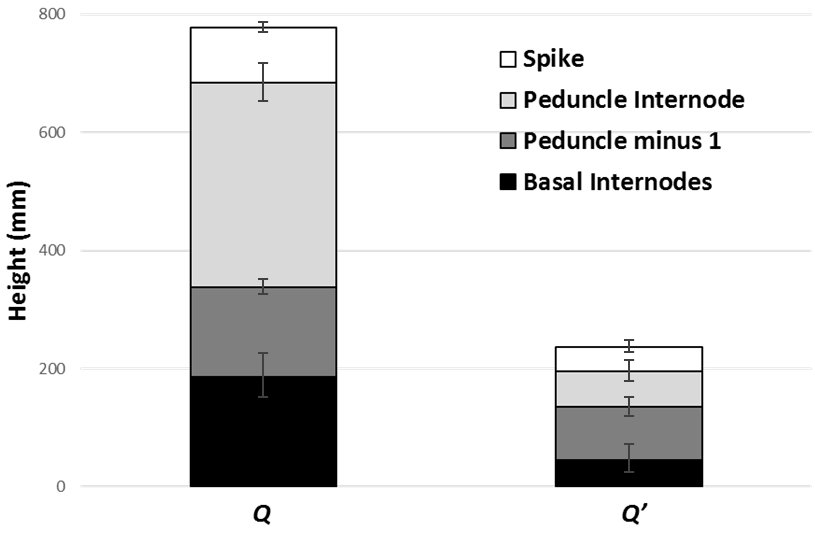

Supplementary Figure 1 Internode elongation phenotype of *Q'*. Total height of *Q'* mutant and its sibling line containing the normal *Q* domestication allele with total height being shown as stacked histogram of average spike, peduncle internode, peduncle minus 1 and remaining basal internode lengths. n= 12 plants. The number of basal peduncle internodes varied between two and three visible internodes amongst measured plants. The length of peduncle and peduncle internode were measured individually as differences in the length of these internodes, as well as the spike, accounted for most of the height reduction in *Q'* plants.

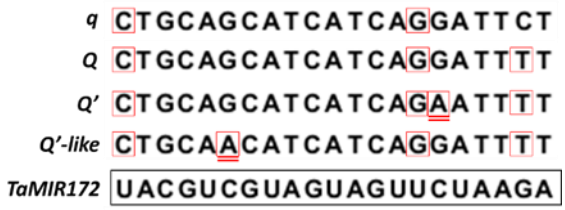

Supplementary Figure 2 miRNA-binding site alignments of pre-domesticated *q*, domesticated *Q*, gain-of-function alleles *Q' and Q'-like*. miRNA-binding site alignments and complementary *miRNA172* with mismatches shown in red and induced mismatches shown by red double underline.

Supplementary Figure 3 The loss-of-function *Q'-Rev1* is difficult to thresh A mechanical thresh test was performed by applying downward pressure to whole spikes with a hand threshing tool before sliding the tool horizontally. SS-like plants containing the domestication allele *Q* had spikes that were easy to thresh and *Q'* plants had spikes that were very easy to thresh with all grain separating from the head leaving an intact rachis. In contrast, *Q'-Rev1* plants had spikes that were firm and required more pressure to thresh with some grain not separating from the spikelets. In addition, the rachis of *Q'-Rev1* spikes had a greater tendency to break into individual nodes/spikelets. In each image the threshed rachis and intact spikelets have been arranged on the left hand side of the image. In *Q* and *Q'* plants, no grain remained bound in spikelets unlike *Q'-Rev1*.

Supplementary Figure 4 The *Q'* mutant reduces the number of basal rudimentary (sterile) spikelets and produces fertile spikelets at basal rachis nodes that are unfilled in *Q* and the loss-of-function mutant *Q'-Rev1*. A, Basal portion of *Q, Q'* and *Q'-Rev1* spikes. Rachis nodes with rudimentary spikelets (those lacking developed florets) are marked *. Scale bar= 1cm. **B,** The average number of infertile spikelets (those that produced no grain) and the number of infertile spikelets which appeared to be rudimentary (without florets) in the basal portion of the main spike of *Q, Q'* and *Q'-Rev1* plants. n= 10. ** $P < 0.01$

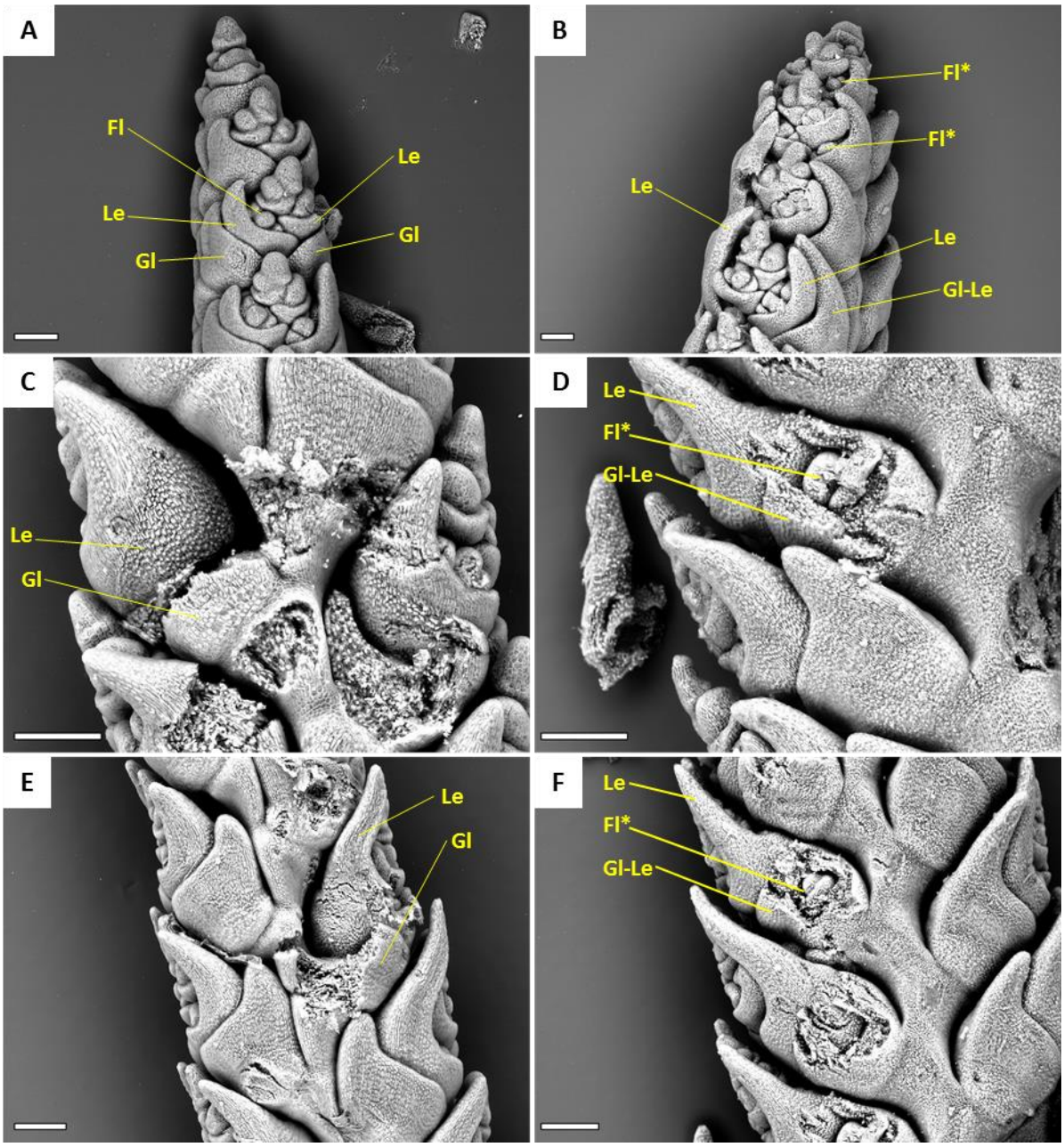

Supplementary Figure 5 Ectopic florets are produced in *Q'* spikelets. SEMs of *SS-like* (Left: **A, C, E**) and *Q'* (Right: **B, D, F**) spikes. Outer-most bracts have been removed from selected spikelets in **C, D, E, F** to reveal structures beneath. In the case of *Q'* ectopic florets (Fl*) are visible beneath the outermost bracts of apical **B,** and dissected **D, F,** spikelets, while the outer-most bracts (glumes) of *SS-like* plants **A, C, E** feature typical sterile glumes. Scale bars= 200µm

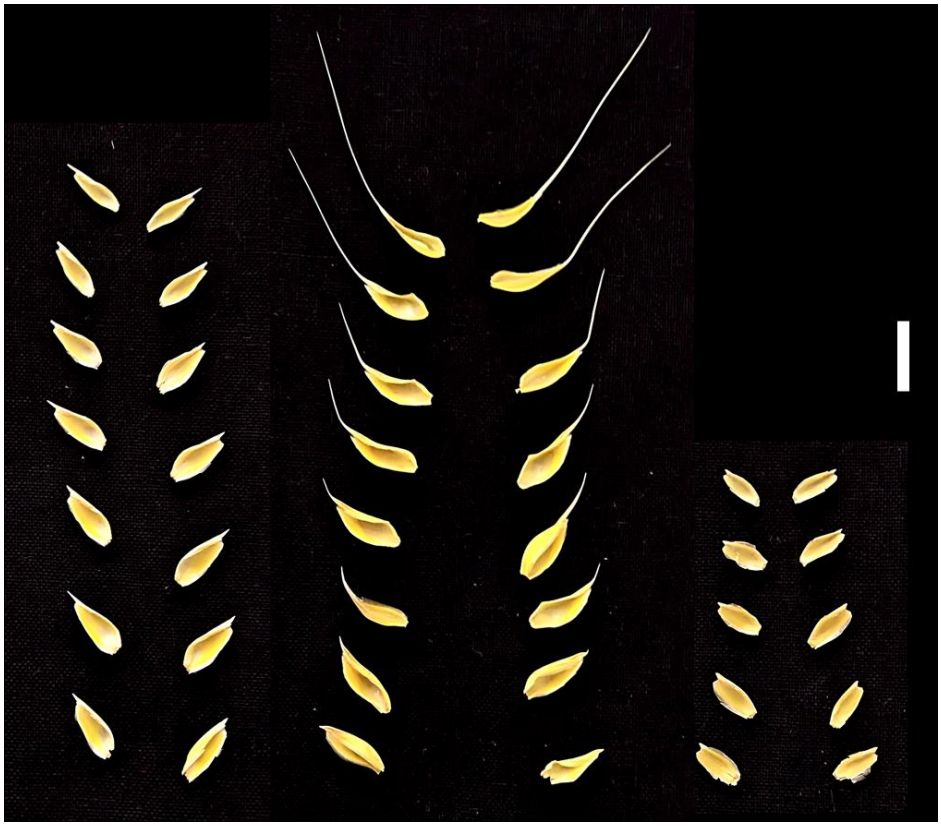

Q ***Q'*** ***Q'-Rev1***

Supplementary Figure 6 Glumes of *Q'* mutant appear lemma-like with awns present in increasing length toward the apical portion of the spike. Glumes of *Q*, *Q'* and *Q'-Rev1* plants removed from one side of asingle spike and placed in order to reflect their position on an intact and upright spike. Note that glumes of *Q'*, or the outermost positions on spikelets which should be occupied by glumes, are only simmilar to the glumes of *Q* when comparing basal spikelets. Scale bar= 1cm

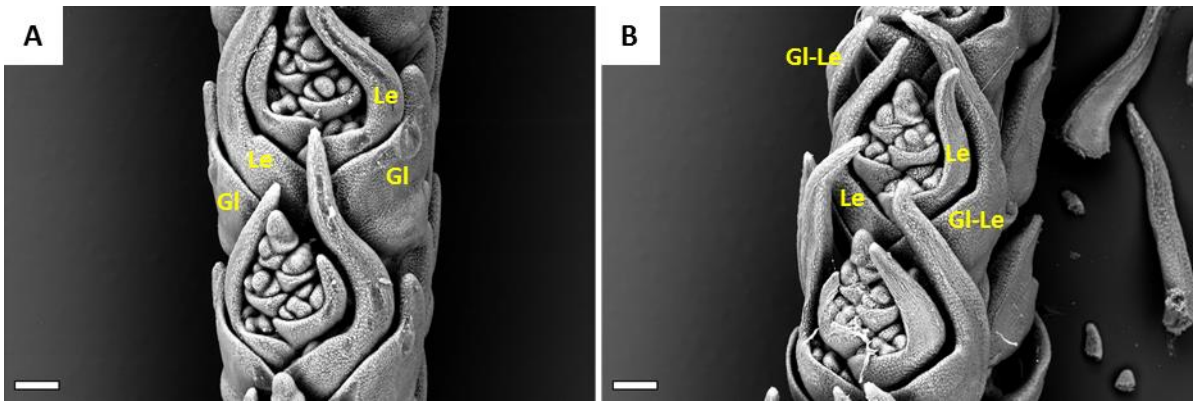

Supplementary Figure 7 Outer most bracts of *Q'* spikelets exhibit elongation of tips as in lemmas. SEMs of spikes shown are at comparable stages of inflorescence development when the tips of lemmas (awns) are beginning to elongate in both *SS*-like (*Q*) and *Q'* plants. The outermost bracts of *Q'* spikelets **B,** feature elongating tips much like a lemma at this stage whereas the outermost bracts of *Q* spikelets **A,** do not elongate and maintain short tips until maturity. See also **S Fig 5.** Gl= glume, Le= Lemma and Gl-Le= Glume-Lemma**.** Scale bars= 200µm

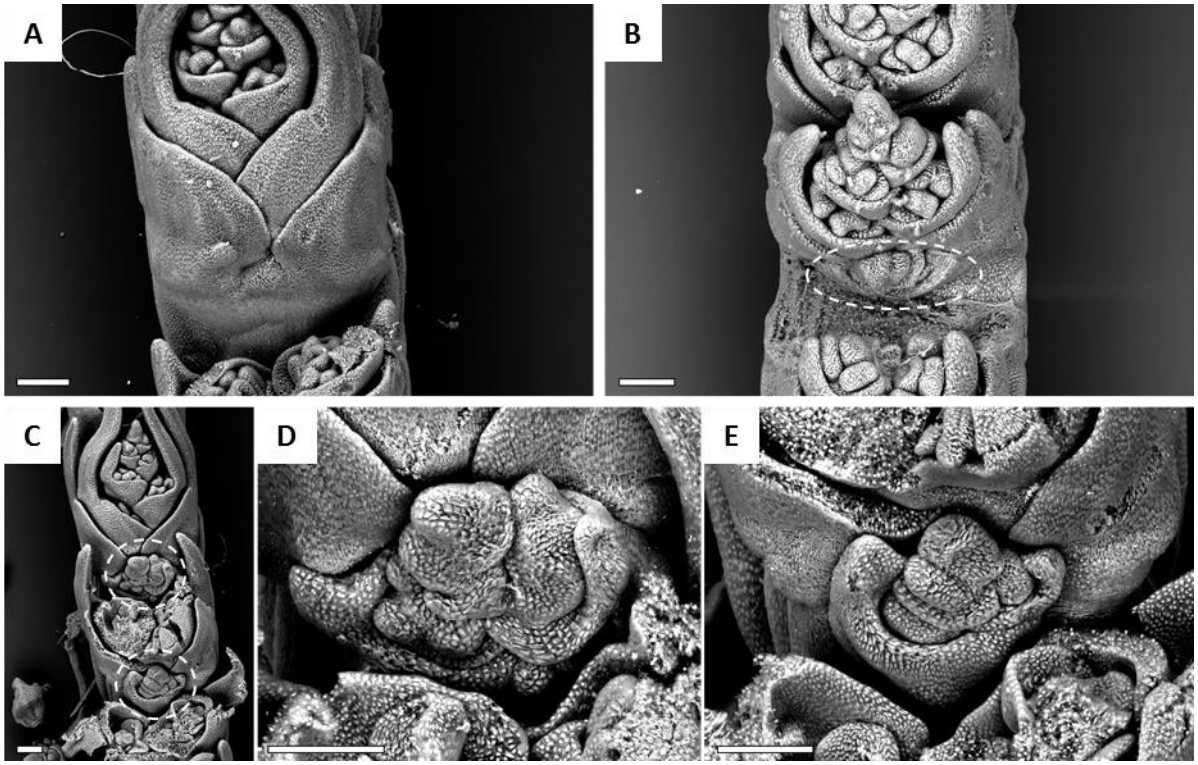

Supplementary Figure 8 Pairs of spikelets form at the central rachis nodes of *Q'* spikes. SEMs of dissected *SS-like* (*Q*) **A,** and *Q'* spikes **B, C, D, E.** to reveal the base of selected spikelets where spikelet pairs form, the spikelet beneath has been removed. The base of the *SS-like* spikelet shown in **A,** represents a typical single spikelet formation. The base of *Q'* spikelets in **B** and **D** show the formation of additional, or paired spikelet at the base of other spikelets. Scale bars= 200µm

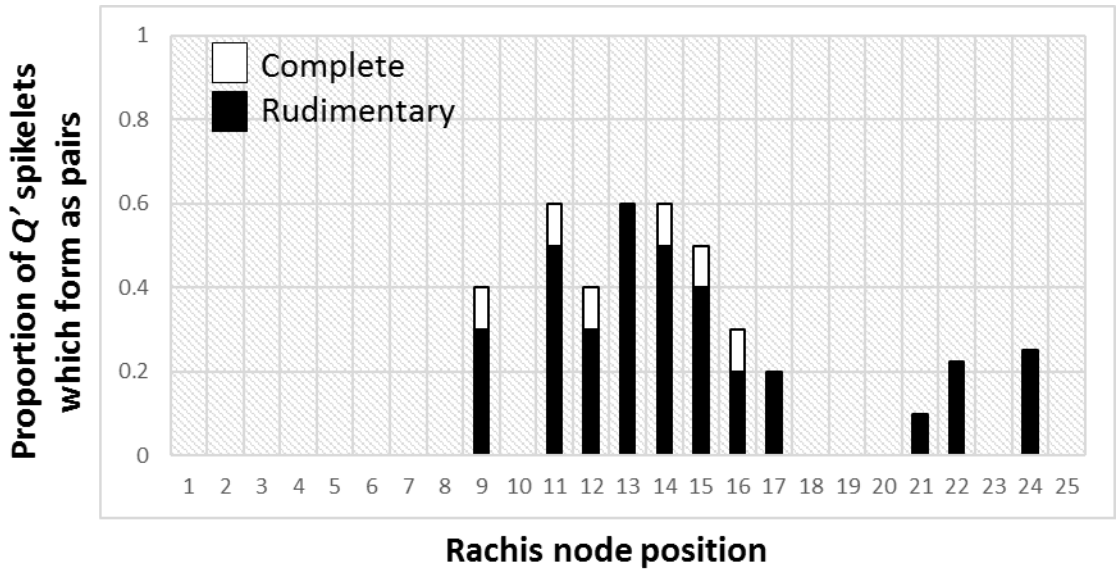

Supplementary Figure 9 Proportion of paired spikelets in *Q'* plants forming at each rachis node. Paired spikelets at specific rachis node positions in *Q'* plants are shown as proportion of all spikelets scored at that rachis node position in main spikes of *Q'* plants. n= 10. Complete paired spikelets contained at least one macroscopic floret.

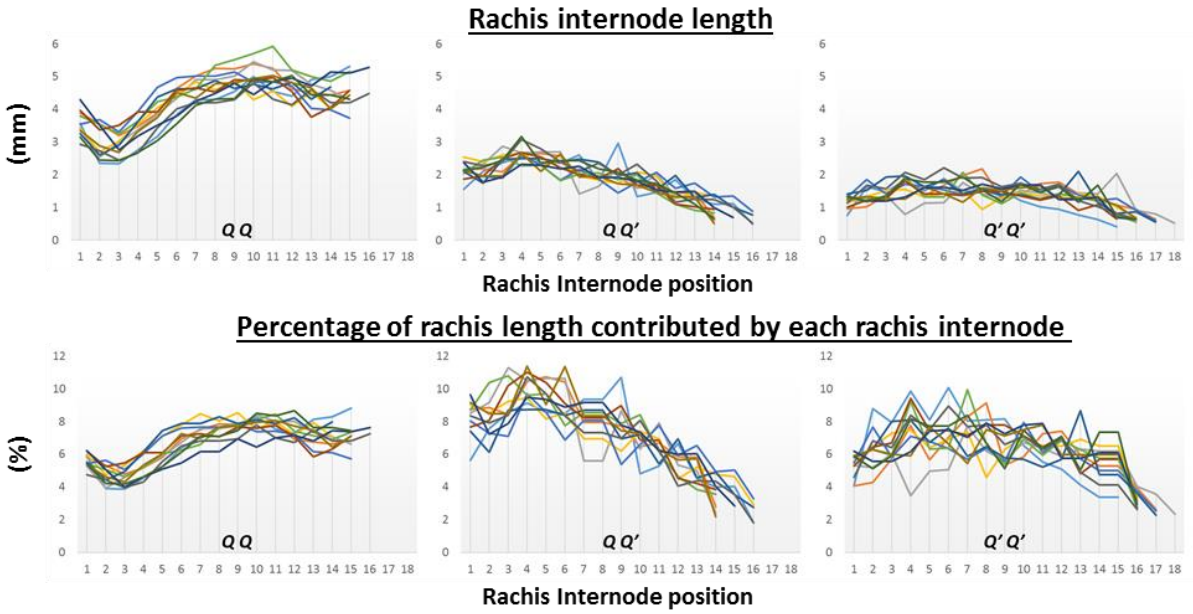

Supplementary Figure 10 Rachis internode elongation is reduced in plants containing the *Q'* with the most severe reduction in internode length occurring at the top of the spike. Rachis internode length profiles of SS-like (*Q Q*), heterozygous (*Q Q'*) and homozygous (*Q' Q'*) mutants where 1 equals the most basal rachis internode of the main spike. n= 12. As rachis internode number varies between individuals, each individual has been plotted and represented by a different color.

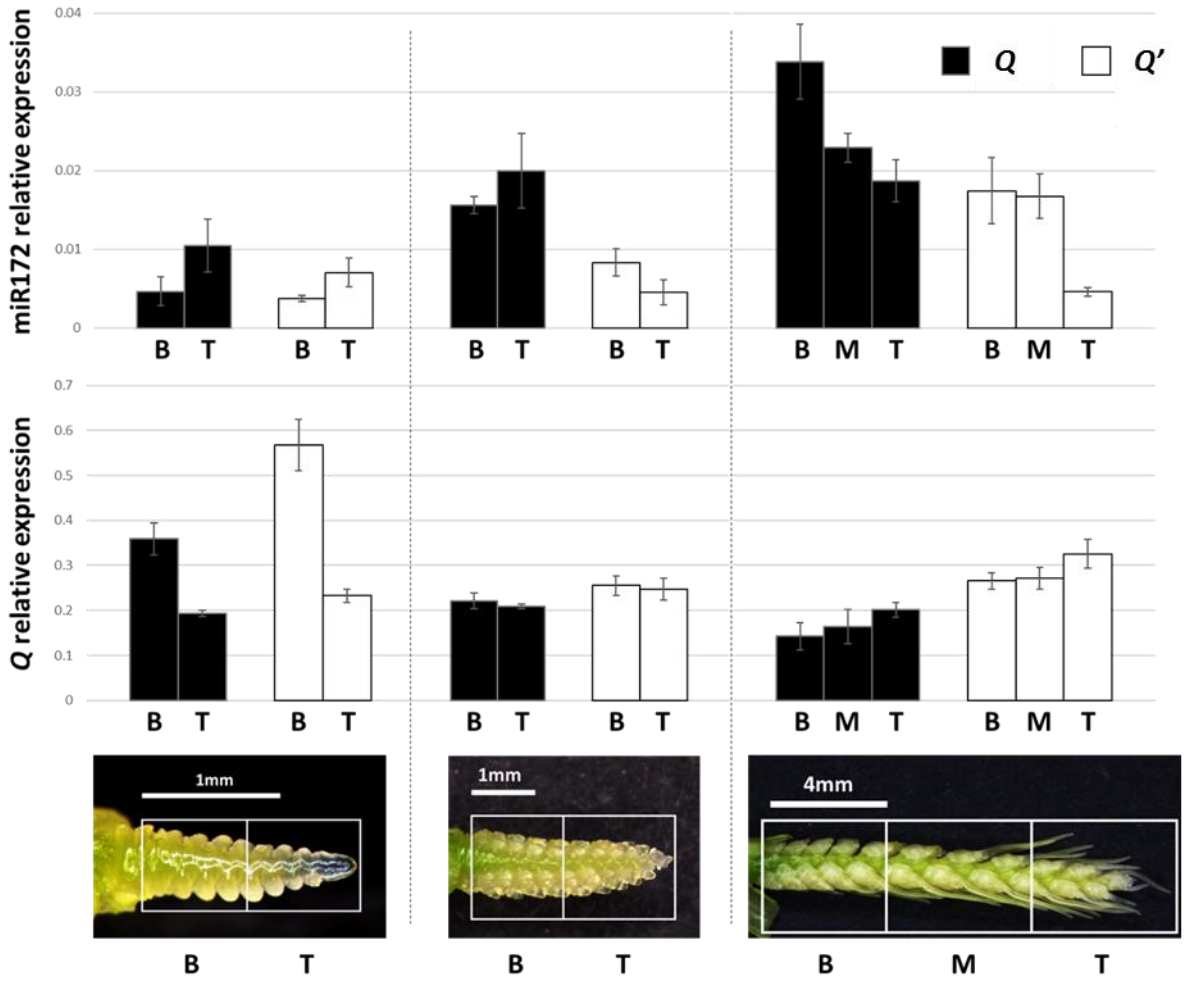

Supplementary Figure 11 Spatial and temporal expression of *Q* and miR172. Images along the bottom of this figure correspond to the developmental stage at which spike sections were harvested. Expression analysis is shown relative to control genes for both *Q* and miR172. Data are presented as mean ± s.e.m of 4 biological replicates in each section, at each timepoint.

Supplementary References

Kosuge, K., Watanabe, N., Melnik, V. M., Laikova, L. I. & Goncharov, N. P. 2011. New sources of compact spike morphology determined by the genes on chromosome 5A in hexaploid wheat. *Genetic Resources and Crop Evolution,* **59,** 1115-1124.

Shaw, L. M., Turner, A. S. & Laurie, D. A. 2012. The impact of photoperiod insensitive Ppd-1a mutations on the photoperiod pathway across the three genomes of hexaploid wheat (Triticum aestivum). *Plant Journal,* **71,** 71-84.

Simons, K. J., Fellers, J. P., Trick, H. N., Zhang, Z., Tai, Y. S., Gill, B. S. & Faris, J. D. 2006. Molecular characterization of the major wheat domestication gene Q. *Genetics,* **172,** 547-555.

Talbot, M. J. & White, R. G. 2013. Methanol fixation of plant tissue for Scanning Electron Microscopy improves preservation of tissue morphology and dimensions. *Plant Methods,* **9,** 36.